

Explosive boiling of liquid nitrogen in a long thin tube and its application to the detection of a local temperature rise

Kazuya Takahata^{a, b, *}

National Institute for Fusion Science^a, National Institutes of Natural Sciences, 322-6 Oroshi, Toki, Gifu, 509-5292 Japan

SOKENDAI (The Graduate University for Advanced Studies)^b, 322-6 Oroshi, Toki, Gifu, 509-5292 Japan

*Corresponding author.

E-mail address: takahata.kazuya@nifs.ac.jp (K. Takahata).

Abstract

To promote the commercial use of high-temperature superconducting devices, the ability to detect temperature anomalies easily and reliably and thereby protect the devices is important. In particular, a sudden local temperature increase due to a superconducting-to-normal transition can damage a device. In the present study, we propose a method to detect explosive boiling of superheated liquid nitrogen sealed in a long thin tube using a pressure gauge connected to the end of the tube. Experiments using a stainless-steel tube with an inner diameter of 1 mm and a maximum length of 50 m under various conditions showed that the local temperature rise caused explosive boiling at a temperature slightly below the superheat limit of 110 K for liquid nitrogen; the results also showed that the rapid pressure increase was transmitted to the end of the tube at approximately the speed of sound (~ 830 m/s). The proposed method of placing a thin tube along high-temperature superconducting conductors or cryogenic structures can be used to easily detect a local temperature rise.

Keywords

high temperature superconducting device

local temperature rise detection

explosive boiling

liquid nitrogen

superheated liquid

1. Introduction

High-temperature superconductors are expected to be used in electrical equipment such as power cables and motors; however, for their widespread use, the ability to detect an accidental temperature rise and protect the equipment will be critical. Thermal runaway in high-temperature superconductors is particularly difficult to detect by electrical methods because it occurs locally [1,2]. Electrical noise further complicates its detection. Therefore, in the present study, we propose a detection method based on the phase transition of cryogenic fluid instead of an electrical method.

In the absence of bubble-forming nuclei, a liquid can remain in a metastable liquid phase even at temperatures greater than its boiling point [3,4]. A liquid in this condition is known as a superheated liquid. However, when the temperature reaches the superheat limit, substantial numbers of bubble nuclei are generated and grow spontaneously in a process known as explosive boiling. According to classical thermodynamics, a spinodal curve divides metastable states from unstable states with respects to small perturbations. For a pure liquid, the spinodal curve is determined by the conditions $(\partial P/\partial V)_T = 0$ and $(\partial^2 P/\partial^2 V)_T > 0$ [5,6]. In practice, however, the liquid loses stability immediately before reaching the spinodal curve because of molecular fluctuations. The kinetic theory of homogeneous nucleation successfully provides the practical superheat limit, and this limit is referred to as the homogeneous nucleation limit [5,6]. For water, our most familiar liquid, numerous experiments have been performed on its metastable superheated phase, beginning in the 1940s [6-9]. In addition, several methods have been developed to measure the superheat limits of other liquids [5,10]; these methods include pulsed-heating [6,9,11-13], capillary-tube [14-20], and bubble-column methods [21-26]. Because the superheat limit differs for different liquids [5], a method that can detect explosive boiling can be used to detect a temperature rise in any temperature range. For high-temperature superconducting devices used at cryogenic temperatures, liquid nitrogen, which has a superheat limit of 110 K at atmospheric pressure [4,5,11,12,14-17], is a good candidate. Cryogenic liquids have fewer impurities (e.g., dissolved gases) that can function as nuclei for bubble formation and can therefore be maintained in a superheated state relatively easily. In addition, to ensure that the superheated state is maintained, the possibility of bubble formation can be further reduced by reducing the liquid/solid contact area. Therefore, the superheat limit of cryogenic liquids has been previously studied using glass capillaries [4,5,14-18]. Glass is used in this application to reduce the number of pits on the solid surface, which is where bubble nuclei form. However, the vapor explosion temperature of cryogenic liquids in copper and stainless-steel tubes has been reported to be approximately the same as that of cryogenic liquids in glass capillaries [4,19].

Previous research has focused on the physical interest of how to bring the measured superheat limit closer to theoretical predictions. To our knowledge, no engineering research on the beneficial use of explosive boiling has been reported. In the present work, we investigate the explosive boiling of liquid nitrogen in a long thin stainless-steel tube to apply it to the detection of a local temperature rise in a high-temperature superconducting device. In previously reported experiments, short capillary tubes have been used; the present work is likely the first time that explosive boiling has occurred using long tubes. If a local temperature rise causes explosive boiling in the tube, the temperature rise at any location can be detected by detecting the pressure rise induced by the explosion. In the experiments in this work, explosive boiling that occurred at a heated location was detected by a pressure gauge installed at the end of a long tube and the temperature at which explosive boiling occurred, referred to here as the explosion temperature, and the propagation speed of the pressure wave were measured. On the basis of the results of these experiments, we discuss whether explosive boiling in a long thin tube can be used to detect a local temperature rise.

2. Experimental procedure

2.1 Experimental setup

Fig. 1 shows a schematic of the experimental setup. The heater unit could accommodate coiled extension tubes of any length at both ends. At the end of extension tube #1 of length $L1$, a 2 m-long extension tube (tube #3) and a pressure gauge were installed. The end of extension tube #2 of length $L2$ was capped. The heater unit and extension tubes #1 and #2 were immersed in liquid nitrogen, and extension tube #3 was extended into the atmosphere. All of the tubes

were made of 316 stainless steel and had an outer diameter of 1.59 mm (1/16 inch) and a wall thickness of 0.3 mm.

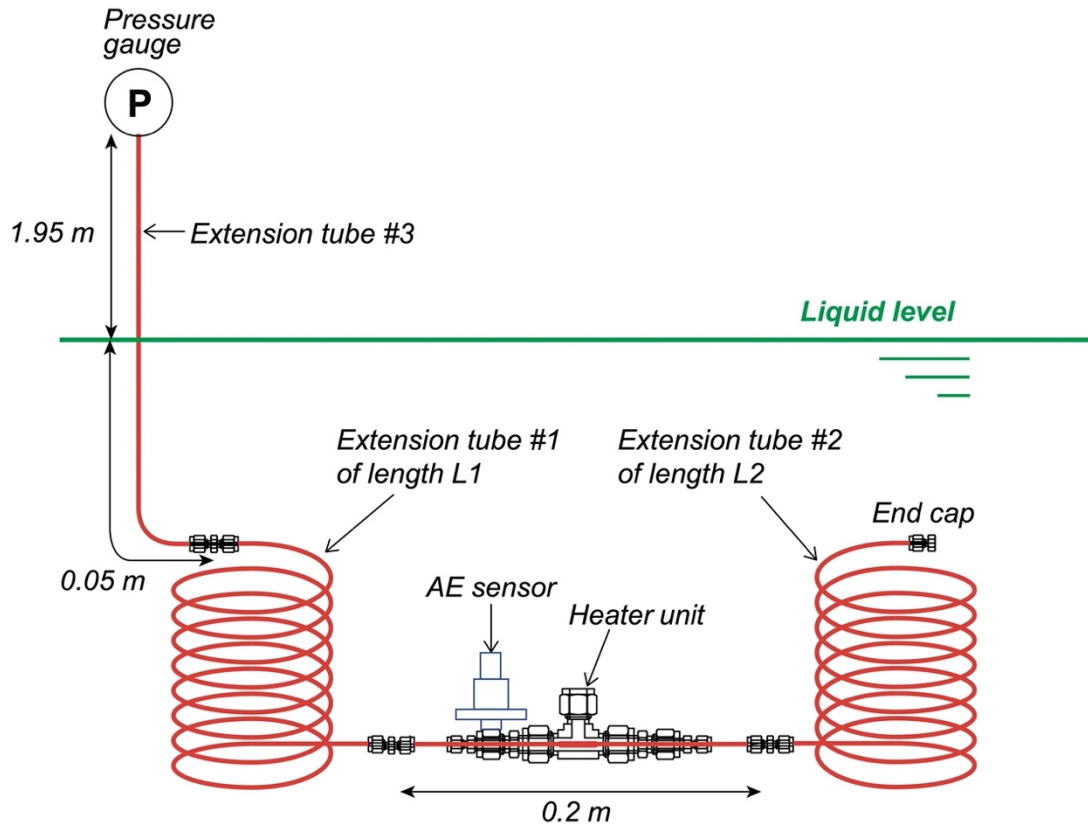


Fig. 1. Schematic of the experimental setup.

Fig. 2 shows the details of the heater unit. A nichrome wire was wound around the center of a 200 mm-long tube to serve as a heater. The length of the heater was 10 mm or 20 mm, and it was used to simulate a local temperature rise of a superconducting conductor. Two copper–constantan thermocouples were attached between the outer wall of the tube and the heater coil. The copper and constantan wires were 0.08 mm thick, with 0.08 mm-thick insulation. A pair of copper and constantan wires was placed parallel along the tube so that the junction was at the center of the heater. A bare copper wire (0.3 mm diameter) was then tightly wound around it before the copper wire was impregnated with solder. Finally, nichrome wire (0.23 mm diameter) was tightly wound around the copper coil. The cold junction of the thermocouple was placed in liquid nitrogen. The thermocouple was calibrated using a separate calibrated thermometer (Cernox model CX-1050, Lake Shore Cryotronics). The calibration experiments were conducted three times to create a calibration curve. The temperature measurement error was ± 0.18 K (standard deviation) in the range from 77 K to 140 K. Two thermocouples were attached to one heater unit. When the rate of temperature change was high, i.e., when the heater power was high, a difference that exceeded the measurement error was observed in the measured values of the two thermocouples. This temperature difference was likely due to a slight difference in the position of the thermocouple junctions. Because compensating for this difference was not feasible, the maximum and minimum measured temperatures are displayed as error bars in the experimental results. To thermally insulate the space around the heater, tube fittings were combined to form a vacuum layer. This layer was piped to a vacuum pump placed in a room-temperature space. Fig. 3 shows the experimental setup. A coiled extension tube (b) was placed

on top of the heater unit (a) and inserted into a tubular liquid-nitrogen dewar (c). The tube drawn from the dewar (d) was connected to the vacuum pump. Liquid nitrogen was poured into the dewar until extension tube #3 (d) was submerged by 50 mm, as shown in Fig. 1.

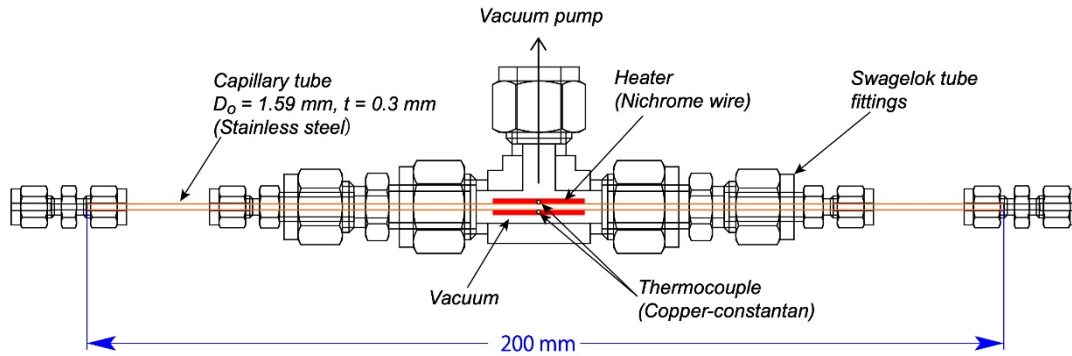


Fig. 2. Details of the heater unit.

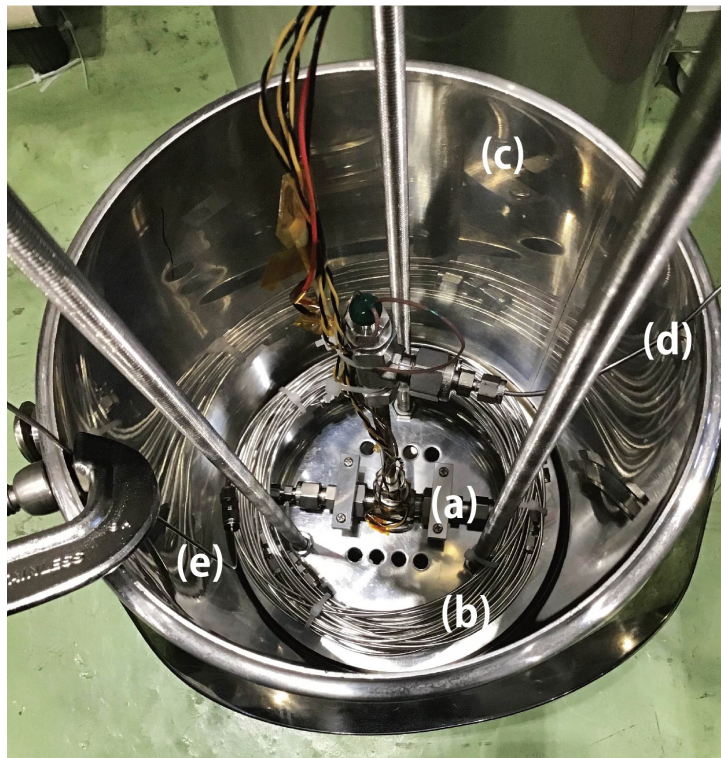


Fig. 3. Photograph of the experimental setup viewed from above: (a) heater unit, (b) coiled extension tube, (c) liquid nitrogen dewar, (d) tube connected to a vacuum pump, and (e) tube connected to a pressure gauge.

Fig. 4 shows the piping diagram, including the valves. The experimental procedure was as follows: (1) V1, V2, and V3 were opened, and the inside of the tube was evacuated to remove impurity gases. (2) V2 was closed, V4 was opened, and nitrogen gas was filled to $\sim 0.5 \text{ MPa}$ via a pressure regulator. (3) Liquid nitrogen was poured into the dewar. (4) At least 30 min was allowed for the pressure to become constant; at this time, the gas in the tube liquefied. (5) The pressure was adjusted to 0.2 MPa using the pressure regulator. (6) When the pressure became constant, V1 was closed to seal the tube. (7) A constant current was applied to the heater; the

heater current was turned off when explosive boiling was detected. (8) At least 5 min was allowed for the pressure and temperature to decrease. (9) V1 was opened. (10) Steps (5) through (9) were repeated.

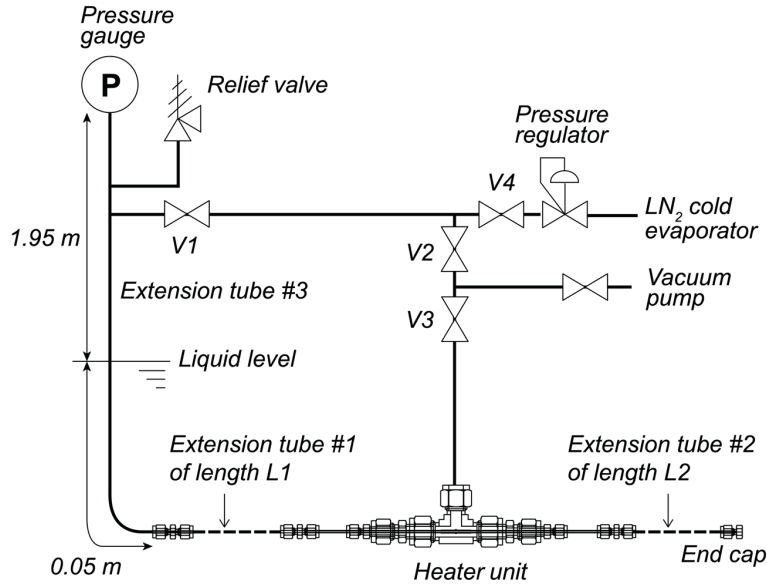


Fig. 4. Piping diagram including valves. (LN_2 : liquid nitrogen)

Impurity gases in nitrogen gas function as bubble nuclei and lead to heterogeneous nucleation; high-purity nitrogen gas from the cold evaporator was therefore used. The initial pressure was set to 0.2 MPa, where liquid nitrogen becomes subcooled, to avoid bubble formation somewhere in the tube as a result of heat input from the surroundings. A relief valve (set at 0.7 MPa) was installed to release the gas at the end of the experiments and to protect the pressure gauge.

The explosion temperature was defined as the measured temperature at the onset of the rapid pressure rise. The pressure gauge was a digital manometer (YOKOGAWA MT210F) with a short time response. The response time was less than 70 ms from the full-scale value (0.7 MPa at gauge pressure) to atmospheric pressure. This response time indicates that a change of 1 kPa, which is necessary to determine the onset of the pressure rise, could be detected in 0.1 ms. The measurement accuracy was $\pm 0.12\%$ of the full-scale value: ± 0.84 kPa. The pressure variation acquired by a data logger was converted into the gradient using the central difference method, and the onset of a rapid pressure rise was defined as when the gradient exceeded a certain threshold.

2.2 Explosion temperature measurements

Preliminary experiments were conducted to determine if the presence of an extension tube would affect the explosion temperature. Specifically, three cases were investigated: a case with no extension tube ($L1 = 0, L2 = 0$), a case with only extension tube #1 with a length of 16 m ($L1 = 16$ m, $L2 = 0$), and a case with only extension tube #2 with a length of 16 m ($L1 = 0, L2 = 16$ m). For $L2 = 0$, the end of the heater unit was directly capped. The effect of heater power was examined at the same time. The heater power was measured by the four-terminal method. The measurement accuracy for the heater power was ± 0.1 W. Experiments under the same conditions were repeated three times each.

2.3 Pressure propagation velocity measurements

The time required for detection after explosive boiling occurs is important from an application perspective. Therefore, the moment when the explosive boiling occurred was detected using an acoustic emission (AE) sensor and the time delay until the pressure changed at the position of the pressure gauge was measured. AE sensors can detect elastic waves with a relatively high frequency of 10 kHz or higher and are mainly used for non-destructive testing of materials. In the experiment, AE signals were confirmed to also be generated by explosive boiling. The AE sensor for cryogenic applications (NF Corporation, AE-901DL) was mounted onto the tube fitting used to create the vacuum layer of the heater unit (Fig. 1). Because the distance between the heater and the AE sensor was ~ 50 mm, the elastic waves from explosive boiling would reach the sensor in 0.01 ms if the speed of sound in stainless steel is assumed to be 5000 m/s. The pressure and AE signals were measured at a frequency of 1 kHz, and the onset was determined from the gradient of the data. Although the measurement frequency was smaller than the frequency of the AE signal, the onset was determined without problem. From the measurement frequency, the measurement accuracy in time delay was less than 2 ms. The length of extension tube #1 was varied to a maximum of 50 m. The end of the heater unit was directly capped without adding extension tube #2 ($L_2 = 0$). The heater length was 10 mm. The pressure propagation velocity was calculated from the measured time delays and the length of extension tube #1 (L_1). Experiments under the same conditions were repeated six times each.

3. Results and discussion

3.1 Explosion temperature

Fig. 5 shows typical time evolutions of the temperature and pressure. The two subfigures show experiments conducted with different input powers applied to the 20 mm-long heater: 1 W (Fig. 5a) and 5.7 W (Fig. 5b). The heater power of 5.7 W was the highest power used in a series of experiments. The results obtained under the three conditions with and without the extension tube are shown together in Fig. 5. Heating was started at 5 s (horizontal axis). The temperature increased with the onset of heating, and a constant pressure of 0.2 MPa was detected at the saturation temperature, 84 K. When the temperature reached ~ 110 K, a sudden pressure increase to ~ 0.3 MPa was observed. Given that the superheat limit of liquid nitrogen is 110 K, this pressure change was clearly due to explosive boiling of superheated liquid nitrogen. When an extension tube was added, the explosive boiling occurred in the same manner. The temperature change after the explosive boiling is governed by two processes: the heat removal by vaporization, which lowers the temperature of the tube, and the thermal insulation by a vapor film, which raises the temperature of the tube. The downward temporary change in temperature during explosive boiling, especially noticeable at $L_1 = 16$ m and $L_2 = 0$, is likely due to the heat removal by vaporization.

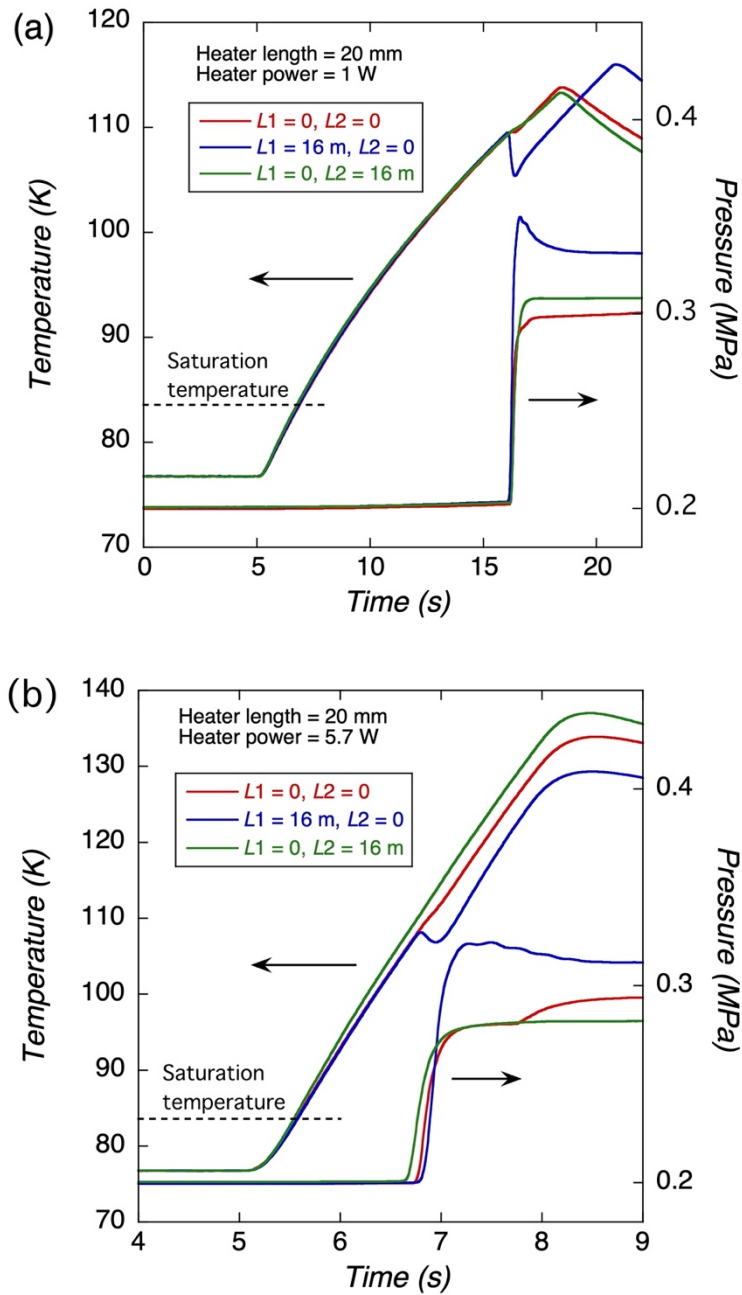


Fig. 5. Time evolutions of temperature and pressure. The two figures show experiments with different input powers applied to the 20 mm-long heater: (a) 1 W and (b) 5.7 W. Heating was started 5 s after the start of the measurement. After the heating was stopped, a decrease in temperature was observed.

Fig. 6 shows the heater-power dependence of the explosion temperature for all of the investigated conditions. As the heater power was reduced, the explosion temperature increased, approaching the superheat limit of 110 K. The presence of the extension tube had little effect on the explosion temperature. The dependence of the explosion temperature on the heater power was greater in the case of the 10 mm heater length (circles in the figure) than in the case of the 20 mm heater length (triangles).

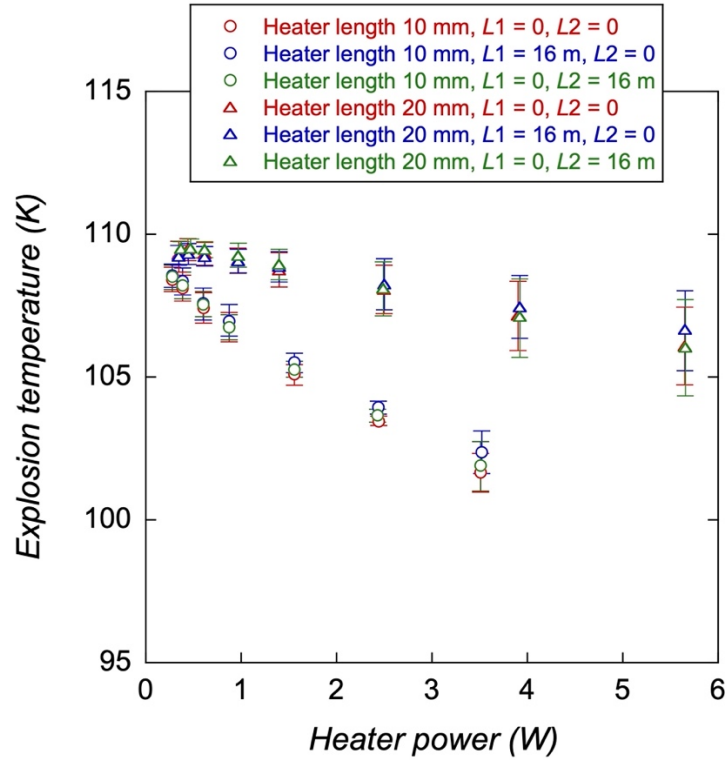


Fig. 6. Heater power dependence of the explosion temperature. The experiments were conducted with two different heater lengths: 10 mm (circles) and 20 mm (triangles). The error bars indicate the maximum and minimum explosion temperatures under the same conditions.

If the heater power is high or the heater length is small, a temperature gradient arises inside the liquid and heterogeneous nucleation can occur instead of homogeneous nucleation. To clarify this point, we used the finite element method to calculate the temperature distributions immediately before the explosive boiling. The software used was Thermal Analysis Toolkit, TDiff 8.0 by Field Precision LLC [27]. For dynamic solutions, the software uses the time-centered Dufort-Frankiel method to advance the diffusion equation. The Neumann condition is applied to the boundary. An example of the calculation results is shown in Fig. 7. A two-dimensional cylindrical geometry was created on the basis of the actual size. Cylindrical systems have variations in R and Z with azimuthal symmetry. For symmetry in the longitudinal direction, the center of the heater was set to $Z = 0$. The outer surface of the geometry was thermally insulated, and the geometry had four regions: liquid nitrogen, stainless-steel tube, copper coil impregnated with solder, and nichrome coil. The liquid nitrogen was assumed to be stationary. Temperature dependence was considered for specific heat and thermal conductivity. Heat was only generated in the region of the nichrome coil. In reality, two thermocouple wires with a diameter of 0.24 mm were sandwiched between the copper coil and the stainless-steel tube; however, they were ignored in this calculation. Fig. 7 shows the temperature distribution immediately before the explosive boiling when heating at 2.5 W with the 20 mm-long heater. The calculated temperatures are consistent with the experimentally measured temperatures, even when the heater power was changed (Fig. 8). The temperature distributions in the radial direction at the center of the heater (R direction at $Z = 0$ in Fig. 7) immediately before the explosion are shown in Fig. 9. When the heater power was 5.7 W, the temperature increased to only 92 K at the center of the tube, even though the inner wall of the tube was 106 K. In this situation, bubble nuclei should be generated near the wall, which is likely to result in

heterogeneous nucleation. When the heater power is low, the temperature distribution in the liquid is narrow and nucleation should be less affected by the wall. Although a few papers with discussions of the effect of walls on explosion temperatures have been reported, Ref. [12] reported experimental results showing that the heating rate and the roughness of the heated surface affect the explosion temperature in liquid nitrogen.

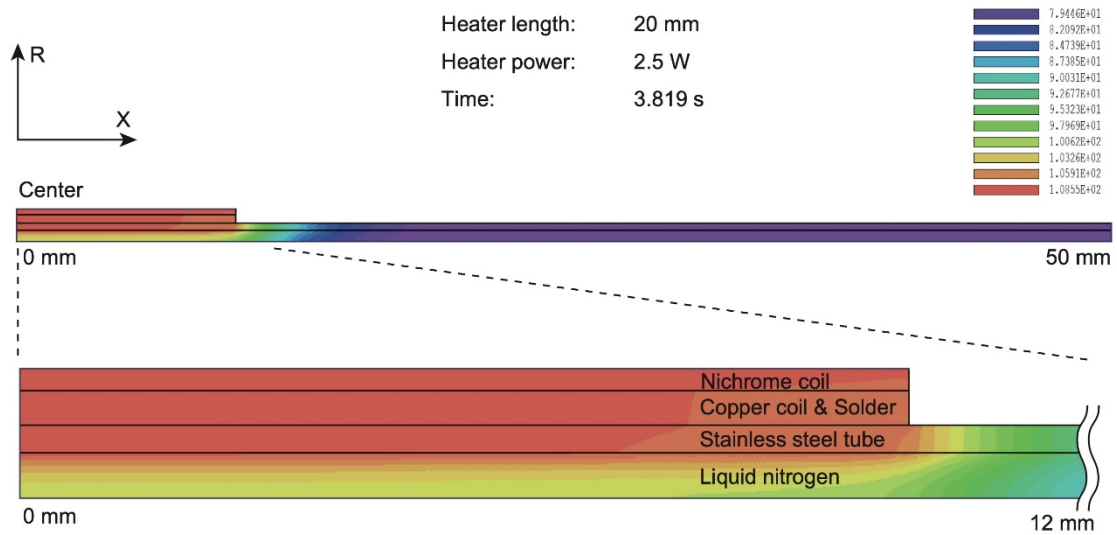


Fig. 7. Example of the calculation of the temperature distribution immediately before explosive boiling using the finite element method. The lower figure is an enlarged view of the upper one.

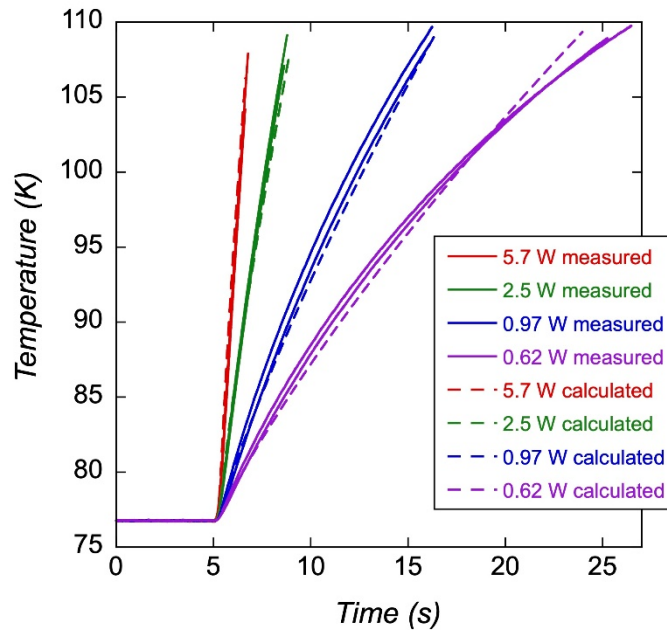


Fig. 8. Measured and calculated temperatures at various heater powers. The two solid lines of the same color show the maximum and minimum measured temperatures in a series of experiments.

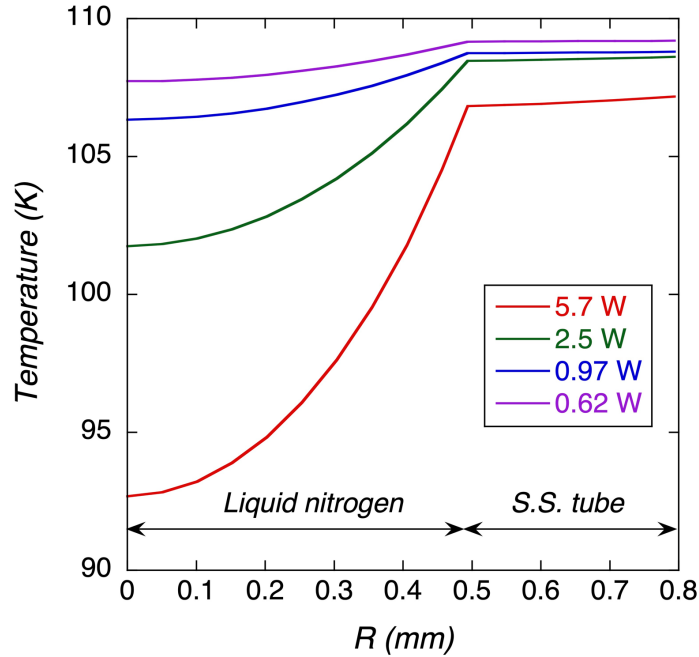


Fig. 9. Temperature distributions in the radial direction at the center of the heater immediately before the explosion. (S.S.: stainless steel)

3.2 Pressure propagation velocity

Assuming that the tubes will be aligned with superconducting cables or conductors, a tube that is several hundred meters long will have to be used. In this case, the time delay for the local pressure increase due to explosive boiling to be transmitted to the pressure gauge at the end of the tube becomes problematic. Therefore, we measured the pressure propagation velocity by adding an AE sensor. The AE sensor attached to the heater unit could detect explosive boiling without a time delay. A typical observation is shown in Fig. 10, where a time delay occurred between the onset of the AE signal and the onset of the pressure change. Fig. 11 shows the measured time delays as a function of tube length $L1$. Six experiments were conducted for each length. The time delay was linearly proportional to $L1$ and was 23 ms when $L1 = 0$. The pressure propagation velocity was calculated by linear regression to be 827 m/s. According to Ref. [28], the speed of sound in liquid nitrogen is 855 m/s. The pressure propagation velocity was therefore close to the speed of sound. This result suggests that, even if explosive boiling occurs at a distance of 1 km, it can be detected in ~ 1 s. Notably, the speed of sound is reduced by the presence of bubbles. Liquid nitrogen inside a tube must be sufficiently subcooled by increasing the initial pressure. In the experiment, liquid nitrogen at a pressure of 0.2 MPa was subcooled to 77K. The degree of subcooling was 7 K.

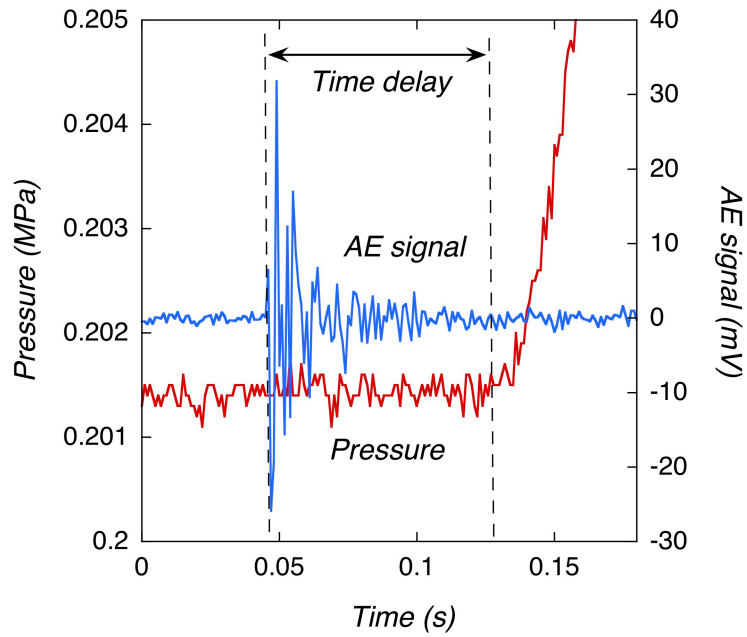


Fig. 10. Time evolution of the AE signal and pressure at the start of explosive boiling ($L1 = 50$ m, $L2 = 0$). The time delay was defined as the time difference between the onset of the AE signal and the onset of the pressure change.

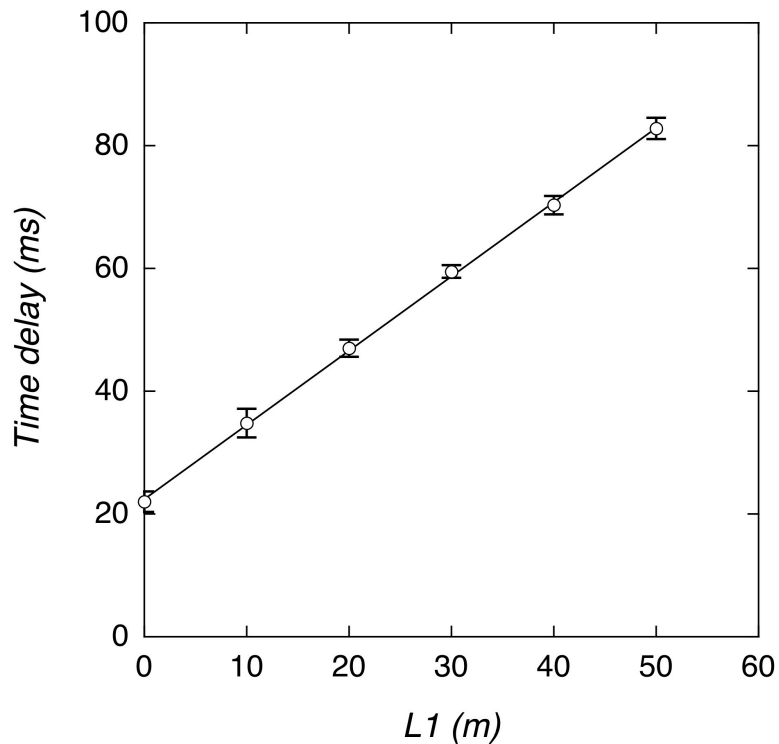


Fig. 11. Measured time delays as a function of the length of extension tube #1, $L1$. The error bars indicate the standard deviation ($n=6$).

The time delay of ~20 ms for $L1 = 0$ is attributed to the 2 m-long extension tube (tube #3). The inside of this extension tube was filled with gaseous nitrogen, and a liquid level was formed at the bottom. The pressure in the liquid was assumed to be transmitted to the gas phase by movement of the liquid level. The observed time delay likely occurred during this process. Although a detailed investigation of the phenomenon is necessary, this delay time is acceptable for practical use.

3.3 Application to superconducting devices

If a thin stainless-steel tube can be placed along a superconducting conductor with which it makes thermal contact, the local temperature rise due to the superconducting-to-normal transition can be detected by the method proposed in the present work. However, this approach raises concerns about reducing the current density of the conductor. For example, a 1 kA conductor with a current density of 200 A/mm² has a cross-sectional area of 5 mm². When this conductor is combined with the 1.6 mm-diameter tube used in the present study, which has a cross-sectional area of 2 mm², the current density is reduced by 30% by simple calculation. The 1.6 mm-diameter tube can be incorporated into power cables and large-current-capacity conductors such as those used for fusion magnets because such conductors have a relatively low current density and can tolerate a decrease in current density resulting from the attachment of a tube. If the diameter of a tube could be reduced, it could be used with thinner conductors. This topic is an issue for future investigations. Of course, the proposed approach can also be used to detect temperature anomalies in cryogenic structures as well as in conductors.

The decrease in explosion temperature due to heterogeneous nucleation (Fig. 6) will likely depend on the diameter and material of the tube. Because this decrease is difficult to predict theoretically [4], it needs to be verified by experiments. Under the experimental conditions used in the present study, the explosion temperatures were between 100 K and 110 K. The proposed approach can therefore be used to detect a temperature rise in high-temperature superconducting devices operating at 77 K.

Because the superheat limit is determined by the nature of a liquid, the detection temperature can be varied by changing the substance used in the tube. The liquid nitrogen used in the present study had a superheat limit of 110 K, whereas hydrogen, neon, and oxygen have superheat limits of 28 K, 38 K, and 134 K, respectively [5,14-17]. Changing the liquid in the tube according to the temperature of the refrigerant used to cool cryogenic equipment would enable a local temperature rise to be detected using explosive boiling.

4. Conclusions

Liquid nitrogen was sealed in a long thin stainless-steel tube with a maximum length of 50 m. The tube was heated at different locations with a heater 10 mm or 20 mm in length to induce explosive boiling, which was detected by a pressure gauge at the end of the tube. The explosive boiling occurred reproducibly at a temperature slightly below the superheat limit of 110 K for liquid nitrogen. The explosion temperature was affected by both the length of the heater and the heating rate, likely because of heterogeneous nucleation caused by the temperature distribution of the liquid nitrogen in the tube. The measured propagation velocity of the pressure increase due to explosive boiling was similar to the speed of sound in liquid nitrogen. These results suggest that, if a thin tube filled with cryogenic liquid can be placed along a superconducting conductor, the local temperature rise that occurs during the superconducting-to-normal transition can be detected quickly and easily.

Acknowledgments

This work was supported by JSPS KAKENHI Grant Number JP19K04340.

References

- [1] Badel A, Rozier B, Takahashi K, Awaji S. Simulation of local dissipation phenomena in the REBCO insert of the 25-T CSM magnet: understanding and preventing destructive thermal runaway. *IEEE Trans Appl Supercond* 2019;29:4600605.
- [2] Badel A, Okada T, Takahashi K, Fujita S, Miyazaki H, Ioka S, Awaji S. Detection and protection against quench/local thermal runaway for a 30 T cryogen-free magnet. *IEEE Trans Appl Supercond* 2021;31:4700705.
- [3] Skripov VP. Metastable states. *J Non-Equilib Thermodyn* 1992;17:193-236.
- [4] Baidakov VG. Explosive boiling of superheated cryogenic liquids. Weinheim: WILEY-VCH Verlag GmbH & Co. KGaA; 2007.
- [5] Avedisian CT. The homogeneous nucleation limits of liquid. *J Phys Chem Ref Data* 1985;14:695-729.
- [6] Hasan MN, Monde M. Review of homogeneous nucleation boiling phenomena under non-equilibrium heating condition and a generalized model for boiling explosion. *Trends Heat Heat Mass Transfer* 2013;13:1-26.
- [7] Briggs LJ Maximum superheating of water as a measure of negative pressure. *J. Appl Phys* 1955;26:1001-1003.
- [8] Zheng Q, Durben DJ, Wolf GH, Angell CA. Liquid at large negative pressures: Water at the homogeneous nucleation limit. *Science* 1991;254:829-832.
- [9] Glod S, Poulikakos D, Zhao Z, Yadigaroglu G. An investigation of microscale explosive vaporization of water on an ultrathin Pt wire. *Int J Heat Mass Transfer* 2002;45:367-379.
- [10] Everhart JG. The thermodynamic and the kinetic limits of superheat of a liquid. *J Colloid Interface Sci* 1976;56:262-269.
- [11] Sinha DN, Brodie LC, Semura JS. Liquid-to-vapor homogeneous nucleation in liquid nitrogen. *Phys Rev B* 1987;36:4082-4085.
- [12] Shiotsu M, Hata K, Sakurai A. *Adv Cryog Eng* 1990;35:437-445.
- [13] Vinogradov VE, Pavlov PA, Biadakov VG. Explosive cavitation in superheated liquid argon. *J Chem Phys* 2008;128:234508.
- [14] Baidakov VG, Skripov VP. Superheating and surface tension of vapor nuclei in nitrogen, oxygen, and methane. *Russ J Phys Chem* 1982;56:499-501.
- [15] Nishigaki K, Saji Y. The superheat-limit of liquid oxygen and nitrogen at 1 atm. *Jpn J Appl Phys* 1981;20:849-853.
- [16] Nishigaki K, Saji Y. On the limit of superheat of cryogenic liquids. *Cryogenics* 1983;23:473-476.
- [17] Baidakov VG, Skripov VP. Experimental study of cryogenic liquids in the metastable superheated state. *Exp Therm Fluid Sci* 1992;5:664-678.
- [18] Skripov VP, Baidakov VG, Kaverin AM. Nucleation in superheated argon, krypton and xenon liquids. *Physica* 1979;95A:169-180.

- [19] Baidakov VG, Kaverin AM. Superheated of liquid xenon in metal tubes. *J Chem Phys* 2009;131:064708.
- [20] Ermakov GV, Lipnyagov EV, Perminov SA, Gurashkin AL. *J Chem Phys* 2009;131:031102.
- [21] Wakeshima H, Takada K. On the limit of superheat. *J Appl Phys* 1958;29:1126-1127.
- [22] Moore GR. Vaporization of superheated drops in liquids. *AIChE J* 1959;5:453-466.
- [23] Porteous W, Blander M. Limit of superheat and explosive boiling of light hydrocarbons, halocarbons, and hydrocarbon mixtures. *AIChE J* 1975;21:560-566.
- [24] Reid RC. Superheated Liquids. *Am Sci* 1976;64:146-156.
- [25] Shepherd JE, Sturtevant B. Rapid evaporation at the superheat limit. *J Fluid Mech* 1982;121:379-402.
- [26] Shusser M, Weihs D. Explosive boiling of a liquid droplet. *Int J Multiphase Flow* 1999;25:1561-1573.
- [27] Field Precision LLC, TDiff 8.0 Thermal transport with temperature-dependent material and radiation boundaries, <https://www.fieldp.com/manuals/tdiff.pdf> [accessed 26 July 2021].
- [28] Users guide to GASPAK[®], Version 3.35/3.45, Horizon Technologies; October 2007.